ARTICLES

Structural and Spectroscopic Investigations of Blue, Vanadium-Doped ZrSiO₄ Pigments Prepared by a Sol−Gel Route

Silvia Ardizzone,*,† Giuseppe Cappelletti,† Paola Fermo,‡ Cesare Oliva,† Marco Scavini,† and Fabio Scimè†

Department of Physical Chemistry and Electrochemistry, University of Milan, Via Golgi 19, I-20133 Milan, Italy, and Department of Inorganic, Metallorganic and Analytical Chemistry, University of Milan, Via Venezian 21, I-20133 Milan, Italy

Received: August 1, 2005; In Final Form: September 30, 2005

A sol−gel reaction starting from silicon and zirconium alkoxides, in water−ethanol mixtures, was employed to obtain vanadium-doped zirconium silicate powders (zircon). The reactions were performed by modulating both (a) the amount of the vanadium salt in the starting mixture and also (b) the amount of mineralizer (NaF). The products of the sol−gel reaction were calcined at 600, 800, 1000, and 1200 °C. The samples were characterized by X-ray powder diffraction (XRPD), electron paramagnetic resonance spectroscopy (EPR), scanning electron microscopy (SEM), X-ray absorption near-edge spectroscopy (XANES), and diffuse UV−vis−near-IR reflectance spectroscopy. Results from the structural, morphological, and optical characterization are examined and cross-compared to produce a consistent picture of the key factors leading to the formation, growth, and optical properties of the reaction products.

Introduction

Zircon structure-based ceramic pigments have been widely used in the ceramic industry for decades. Zircon offers superior stability at high temperature and in corrosive environments. Furthermore, pigments with zircon as the host crystal yield a wide variety of colors and shades.[1−8] The turquoise blue zircon pigment, which contains vanadium as the dopant, was the first to be introduced commercially and one of the most successful.[9]

It is generally accepted that the origin of the blue color, in this pigment, is due to the solid solution of V^{4+} in the zircon lattice;[10] however the actual location of vanadium in the zircon structure is still unclear and has been the subject of numerous studies, in some cases leading to controversial interpretations. Furthermore, the role played by the addition of a fluxing agent, or mineralizer (halides), in the promotion of the blue color has not yet been fully clarified.

Demiray et al.,[10] on the grounds of optical absorption and X-ray diffraction studies, suggested that V^{4+} is prevailingly located in the distorted dodecahedral zirconium sites; these conclusions appeared to be in agreement with ab initio cluster calculations of the lattice energy.[11] Exactly the opposite conclusion was reached on the basis of energy level calculations, which indicated that V^{4+} preferred the tetrahedral silicon site[12] as did Raman spectroscopy.[13] This was further confirmed by electron paramagnetic resonance (EPR) studies, on the basis of a

spectrum detectable only at $T < 20$ K and with $A_{\parallel} = 88$ G, $A_{\perp} = 31$ G.[12] Indeed, the relatively low values of the hyperfine components were more easily attributable to a tetrahedral (low coordination number) than to a dodecahedral (high coordination number, i.e., more ionic bond).[14] Furthermore, the presence of a dynamic Jahn−Teller exchange could introduce a number of low-lying excited vibronic states through which Orbach relaxation would occur. This could easily explain the fact that the EPR spectrum was not detectable at high temperature.[12] A further possibility some workers have proposed is that both sites can be occupied to a significant extent. This hypothesis was supported by EPR and optical measurements[15] and by lattice energetic calculations[16] which found very little difference in the energy of the V^{4+} occupying either of the two principal lattice sites. More recently, Ocana et al.[17] reached similar conclusions, by using a variety of spectroscopic techniques. These authors suggested that the dopant substitutes both for silicon in the tetrahedral site and to a lesser extent for zirconium in the dodecahedral site. Extended X-ray-absorption fine structure measurements (EXAFS) of the vanadium K edge gave the ratio of the occupancy of the two sites as Nt/Nd = 1.6. This ratio could also be used to rationalize their IR measurements. Furthermore, not only did they observe the above-mentioned low-temperature EPR spectrum attributable to V^{4+} in a tetrahedral site, but, in the presence of large amounts of V^{4+}, they recorded also a second EPR feature at temperatures even above that of liquid nitrogen, formed by a single structureless feature attributable to many V^{4+} ions dipolarly interacting with each other. However, this broad EPR band remained unresolved and could not bring further information.

A further possibility for the site occupancy of the V^{4+} is its insertion into a interstitial, strongly distorted tetrahedrally

---
* Corresponding author. Telephone: +390250314225. Fax: +390250314300. E-mail: silvia.ardizzone@unimi.it.
† Department of Physical Chemistry and Electrochemistry. E-mail: (G.C.) giuseppe.cappelletti@unimi.it; (C.O.) cesare.oliva@unimi.it; (M.S.) marco.scavini@unimi.it; (F.S.) fabio.scime@libero.it.
‡ Department of Inorganic, Metallorganic and Analytical Chemistry. Telephone: +390250314425. E-mail: paola.fermo@unimi.it.

coordinated site.[18] In this case the charge balance could be maintained through silicon vacancies. This latter hypothesis, earlier proposed on the grounds of X-ray investigations on single crystals[18] was further supported by more recent polarized electronic absorption spectroscopy (EAS)[19] and, partially, also by solid-state NMR[20] data which actually suggest a possible third location of vanadium at high metal loadings.

The purpose of this work is to examine the siting of vanadium by numerous structural and spectroscopic techniques and to find a satisfactory explanation which can rationalize the diverse evidence, clarifying also the role played by NaF as the mineralizer.

Experimental Section

Samples were obtained by sol−gel procedure both in the absence and in the presence of increasing amounts of NaF.

All the chemicals were of reagent grade purity and were used without further purification; doubly distilled water passed through a Milli-Q apparatus was used to prepare solutions and suspensions.

Sample Preparation. The zircon samples were prepared by a previously reported sol−gel procedure consisting of two different hydrolysis steps.[4,7,8] At the beginning $Si(OC_2H_5)_4$ (0.20 mol) was added drop by drop to an aqueous solution containing variable amounts of the vanadium(III) salt (VCl_3) previously stirred at 60 °C for about 20 min in order to achieve the complete dissolution of the dopant ion. Then 0.35 mol of ethanol and 0.10 mol of reaction catalyst (HCl) were added to the mixture which was left under rapid stirring for 30 min (i.e., the time of the first hydrolysis step). Subsequently a solution of $Zr(OC_3H_7)_4$ (0.20 mol) and water was added to the mixture. The final suspension was kept under stirring at 60 °C for 2 h (i.e. the time of the second hydrolysis step). The product, cooled at room temperature and was dried in an oven at 60 °C, and then the obtained xerogel was thermally treated at either 600, 800, 1000, or 1200 °C for 20 h.

The first series of samples was prepared by using a variable V/Zr molar ratio (0.00, 0.02, 0.04, 0.06, 0.10, and 0.14). The second series of samples was obtained by using a constant V/Zr molar ratio of 0.10 but adding different amounts of the mineralizer NaF (0.10, 0.20, 0.26, 0.35, 0.52, and 0.70 NaF/Zr molar ratio) before the second hydrolysis step.

The samples are labeled as following: V_xNaF_y800, where x = V/Zr molar ratio, y = NaF/Zr molar ratio, and 800 is the calcination temperature (°C).

Sample Characterization. Room-temperature X-ray powder diffraction (XRPD) patterns were collected between 10 and 80° (2θ range, $\Delta 2\theta = 0.02°$) with a Siemens D500 diffractometer, using Cu Kα radiation. Rietveld refinement has been performed using the GSAS software suite[21] and its graphical interface EXPGUI.[22] The backgrounds have been subtracted using a shifted Chebyshev polynomial. The diffraction peak's profile has been fitted with a pseudo-Voigt profile function. Site occupancies and the overall isotropic thermal factors have been varied. The amorphous content was estimated by means of an internal standard method. The internal standard powder, pure TiO_2, was added in known quantity (10 wt %).

V K-edge (5465 eV) X-ray absorption spectra were collected at room temperature at the BM-8 station (GILDA, experiment no. 08-01-377) at the ESRF synchrotron radiation laboratory (Grenoble, France). The spectra were collected in fluorescence mode, using ion chambers as detectors and a double-crystal Si (111) monochromator, which yielded a resolution of approximately 0.5 eV. To perform the measurements, an amount of sample appropriate to give an edge jump of about 1 in the absorption coefficient was mixed with polyethylene and then pressed to a pellet. Each spectrum was then normalized at ≈1000 eV above the edge, where the EXAFS oscillations were not visible any more. The preedge peaks were overlaid with fittings based on a mixing of Gaussian and Lorentzian functions.

Electron paramagnetic resonance spectra were collected with a Bruker Elexsys instrument, equipped with a standard rectangular ER4102ST cavity and operated at 9.4 GHz, 1 mW microwave power, and 1 G modulating amplitude and in the temperature range of −173 and +25 °C. The intensity of the magnetic field was carefully checked with a Bruker ER35M teslameter, and the microwave frequency was measured with a HP 5340A frequency meter. Spectral simulations, when required, were carried out by means of the Bruker SimFonia program.

The particle morphology was examined by scanning electron microscopy using a Cambridge 150 Stereoscan.

Diffuse reflectance spectra were acquired in the vis−near-IR range from 350 to 1200 nm using a JASCO/UV/vis/near-IR spectrophotometer model V-570 equipped with a barium sulfate integrating sphere. A block of Mylar was used as reference sample following a previously reported procedure.

The color of the fired samples was assessed on the grounds of L^*, a^*, and b^* parameters, calculated from the diffuse reflectance spectra, through the method recommended by the Commission Internationale de l'Eclairage (CIE).[7] By this method the parameter L^* represents the brightness of a sample; a positive L^* value stays for a light color, while a negative one corresponds to a dark color; a^* represents the green (−) → red (+) axis; and b^* represents the blue (−) → yellow (+) axis.

Results

In the following, results will be presented discussing first the samples obtained, in the absence of mineralizer, at variable V content and temperatures (green samples) and subsequently the samples obtained at increasing amount of mineralizer, NaF (blue samples).

Green Samples. *Structural Characterization.* Several attempts are reported in the literature to stabilize the blue color of V-doped zircon pigments in the absence of mineralizers either by using the sol−gel process or adopting high temperatures.[23] Only for very low vanadium loadings and high calcination temperatures a light blue color can be obtained. Otherwise, when no mineralizers are added, a greenish, unsatisfying, color of the pigment is invariably obtained. The dependence of the structural features with the temperature of calcination for the present samples obtained at constant vanadium content (V/Zr = 0.1) is shown in Figure 1. At 600 °C (Figure 1a), the zircon phase is not appreciable and the only crystalline phase is zirconia, mainly present as the tetragonal polymorph. No crystalline phase related to silica can be detected. At 800 °C (Figure 1b), instead, different phases are apparent: the desired phase, zircon, ($ZrSiO_4$), and ZrO_2 mainly in the monoclinic form. By increasing the temperature, besides zircon and monoclinic zirconia, a weak peak at ≈21.0° shows the initial formation of a crystalline phase related to SiO_2, crystobalite. Results in Figure 1 are in agreement with literature data,[1,24] which individuate three steps leading to $ZrSiO_4$ formation: first, crystallization of a phase having the t-ZrO_2 structure; second, a phase transformation from t-ZrO_2 to m-ZrO_2; and third, almost simultaneous to the phase transformation, the reaction between m-ZrO_2 and an amorphous silica rich phase, leading to zircon. Table 1 reports the quantitative phase composition of the powders at the different

22114 *J. Phys. Chem. B, Vol. 109, No. 47, 2005*
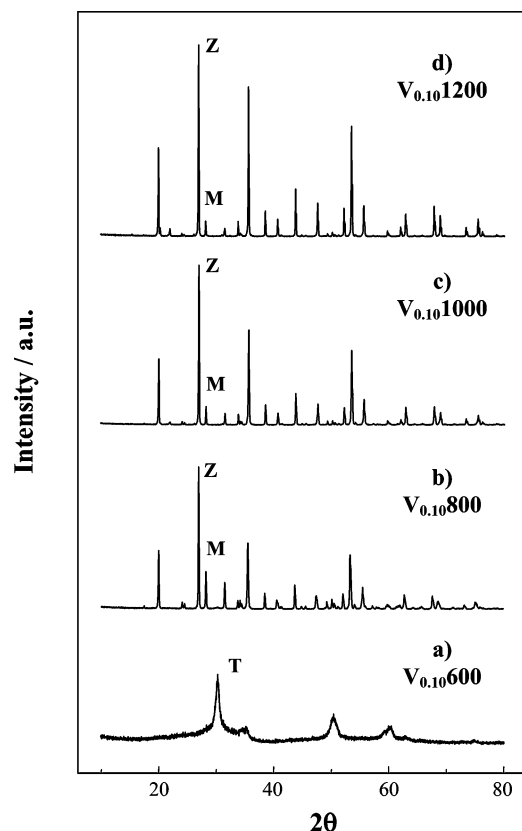
Ardizzone et al.

Figure 1. Powder X-ray diffraction lines of samples at the same V/Zr content calcined at different temperatures in the range of 600−1200 °C: T and M, tetragonal polymorph and monoclinic zirconia (ZrO_2), respectively; Z, zircon ($ZrSiO_4$).

TABLE 1: Quantitative Phase Composition (mass %) of Samples Prepared at the Same V/Zr Molar Ratio (0.1), Calcined at Different Temperatures[a]

sample	% Z_{ZrSiO_4}	% M_{ZrO_2}	% T_{ZrO_2}	% C_{SiO_2}
$V_{0.10}600$		23.6(8)	76.3(2)	
$V_{0.10}800$	76.5(4)	21.9(7)	1.4(9)	
$V_{0.10}1000$	91.5(8)	7.5(4)		0.8(8)
$V_{0.10}1200$	92.5(8)	5.9(7)		1.4(5)

[a] Z = zircon, M = monoclinic ZrO_2, T = tetragonal ZrO_2, and C = crystobalite SiO_2.

temperatures obtained by refining the crystal structures by the Rietveld method.

Figure 2 reports the trend of the unit cell volume as a function of the heating temperature. The figure reports also, for the sake of comparison, the literature unit cell volume of undoped zircon (dashed line),[8] which remains in any case smaller than the cell volume of the V-doped one. This contrasts with the results of Demiray et al.,[10] who reported that the lattice parameters of zircon did not change with V-doping in their investigation. However, Torres et al.[25] as well as Monrós et al.[5] reported expanded cell volumes with V-doped zircon, comparable to those observed in the present case. They interpreted this effect as the result of substituting a larger ion (V^{4+}) for a smaller (Si) one in the zircon tetrahedral positions. Furthermore, the last authors observed[5] a decreasing trend with temperature of the cell volume of V-doped zircon very similar to that observed by us (Figure 2), though somewhat shifted toward slightly lower volumes. In Figure 2 the cell volume approaches the value of the undoped zircon cell when the zircon phase prevails, i.e., according to the XRD spectra of Figure 1, at the higher temperatures. Table 2 reports the results obtained by refining,
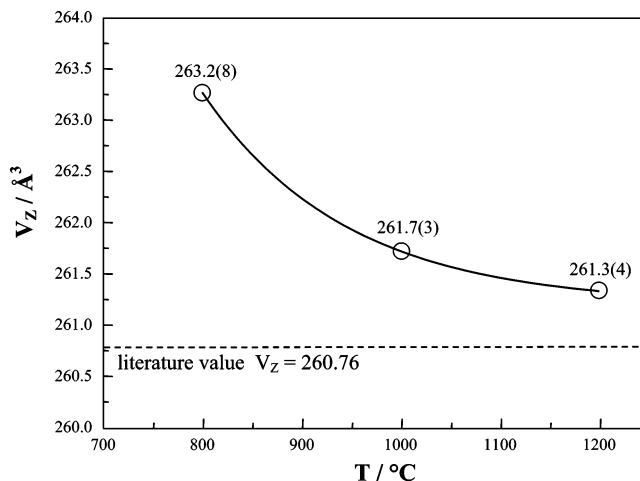

Figure 2. Zircon cell volume as a function of the calcination temperature for a sample with V/Zr = 0.1.

TABLE 2: Quantitative Phase Composition (mass %) and Relative Cell Volume of Samples Prepared at Different V/Zr Molar Ratios, Calcined at 1000 °C[a]

sample	% Z_{ZrSiO_4}	% M_{ZrO_2}	% T_{ZrO_2}	% C_{SiO_2}	% amorphous	$V_Z/Å^3$
$V_{0.00}$		31.9(2)	19.0(2)		49.0(6)	
$V_{0.02}$	11.5(2)	7.8(4)	80.6(4)			261.2(9)
$V_{0.04}$	81.1(8)	15.4(3)		3.3(9)		261.4(6)
$V_{0.06}$	83.8(8)	14.0(0)		2.1(2)		261.4(3)
$V_{0.10}$	91.5(8)	7.5(4)		0.8(8)		261.7(3)
$V_{0.14}$	86.7(5)	10.3(8)		2.8(7)		261.5(1)

[a] Z = zircon, M = monoclinic ZrO_2, T = tetragonal ZrO_2, and C = crystobalite SiO_2.
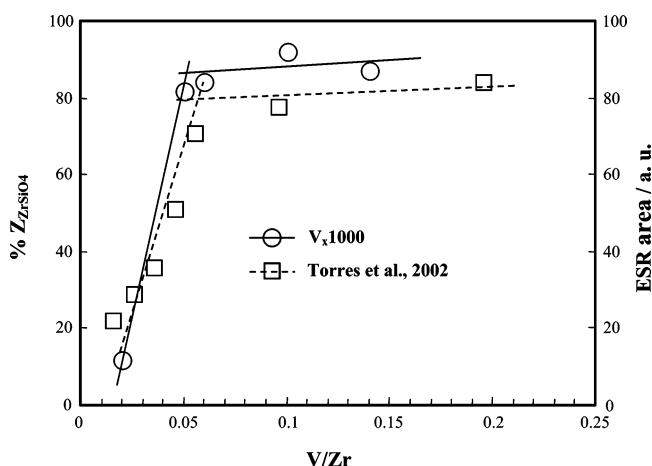

Figure 3. Zircon-phase mass percent (open circles) and ESR peak area from ref 1 (open squares) as a function of the V/Zr content.

by the Rietveld method, the crystal structures of samples obtained at increasing vanadium loadings and heated at 1000 °C. In the absence of the vanadium the only crystalline phases are monoclinic and tetragonal zirconia. No crystalline phases related to silica can be observed, and the sample appears to be still largely amorphous. Upon addition of 0.02 V/Zr molar ratio, instead, different phases are appreciable: the desired phase zircon ($ZrSiO_4$) and ZrO_2 both in the monoclinic and in the tetragonal form. The phase enrichment in zircon increases to about 90% when the amount of V increases to 10%, also accompanied by an increased value V_Z of the cell volume. Then, at even greater amounts of V, both the percent amount of zircon and V_Z decrease slightly, according also to Figure 3.

The role played by the guest metal on the promotion of the zircon lattice is apparent. This effect has been observed
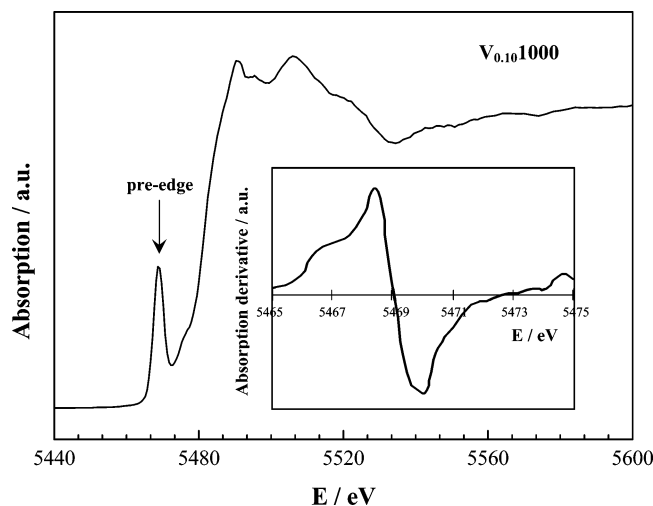
Blue, Vanadium-Doped ZrSiO₄ Pigments

J. Phys. Chem. B, Vol. 109, No. 47, 2005 **22115**

Figure 4. Representative V K-edge XANES spectrum of the $V_{0.10}$-1000 sample. Inset: the derivative plot of the preedge peak.
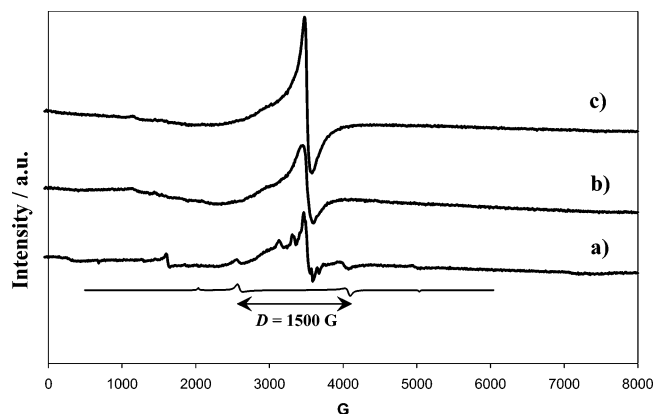

Figure 5. EPR spectra of samples calcined at 1000 °C with V/Zr molar ratio (a) 0.02 (thinner line, simulation), (b) 0.10, and (c) 0.14.

TABLE 3: Spectral Characteristics of Preedge Peak in Samples Calcined at 1000 °C at Different V/Zr Contents

	preedge peak	
sample	energy position (eV)	integral intensity
$V_{0.02}$	5469.4	908.2
$V_{0.04}$	5469.0	902.8
$V_{0.06}$	5469.1	856.4
$V_{0.10}$	5469.3	837.4
$V_{0.14}$	5469.5	803.5

previously in the literature also in the case of other metals (Fe, Pr) doping the zircon lattice.[4,7,8] Several authors interpret this occurrence as being due to the initiator role, played by the guest ion, in the nucleation of the zircon structure within the zirconia lattice.[1] The promotion of the zircon phase appears to increase progressively with the vanadium loading in the samples (Figure 3) up to a content around 0.05% and then to level off for higher values. Several authors report "solubility limits" for vanadium in the zircon structure, in the absence of mineralizers, which can vary from 0.01 [25] to 0.05,[1] depending on the parameter followed. For the sake of comparison Figure 3 reports, together with the present results, also data from the literature[1] obtained as relative areas of the ESR signal at 10 K. The two sets of data appear to be in excellent agreement notwithstanding the totally different basis of the data and, jointly, indicate a value around 0.05 molar ratio as the "saturation limit" beyond which the role of vanadium changes.

XANES Spectroscopy. The shape of the XANES spectra provides useful and detailed information on the local structure and coordination geometry of the central vanadium atoms. A characteristic feature of XANES spectra of vanadium compounds is the appearance of a preedge peak due to the so-called 1s→3d transition which is mainly caused by a mixing of the 2p orbitals of the oxygen atoms with the 3d orbitals of the vanadium atoms, and it is allowed only in absence of a inversion center on the V position.[26] The energy position of the preedge peak is related to the formal valence of the central vanadium ion. Wong et al.[26] report a variation of 1.1 eV between the preedge peak energies of V_2O_4 and V_2O_5. Unfortunately in the present determinations, the reported variation in the preedge peak energy is comparable with the energy resolution of the measurements and no attempt was made to obtain indications concerning the oxidation state of vanadium in the different products. The integral intensity of the preedge peak is correlated both to the average length of the V−O bonds and to the symmetry around the V atom. Empirically the strength of this preedge transition is found to depend on the size of the "molecular cage" defined by the nearest neighbor ligands coordinating to the vanadium center.[26−28]

Figure 4 shows the V K-edge XAS spectrum of a representative sample ($V_{0.10}$1000). Closer examination of the spectrum shows that there is a complex structure of the preedge peak features (Figure 4, inset). This structure, which was previously observed in V_2O_3,[26] shows splittings of 1.3 and ca. 2.0 eV. The

splittings in the 1s−3d transition are caused by crystal-field splitting of the ground state.[26]

Table 3 reports the peak integral intensities in the case of the green samples obtained in the absence of mineralizers. For the two lowest vanadium concentrations, the preedge integral intensities only slightly decrease, while they show a sharp drop between 0.04 and 0.06 vanadium loadings. The decreasing trend of the intensity suggests that V progressively occupies lattice positions with higher coordination number or higher symmetry.[26−28] The trend shown by the intensities, i.e., a slight decrease followed by a marked drop at about 0.05, can be compared with the trend shown in Figure 3, where the same vanadium amount (0.05) provoked a sharp variation in zircon-phase structural promotion.

EPR Spectroscopy. The ZrSiO₄ sample doped with 0.02 V/Zr molar ratio shows an EPR spectrum composed of many lines. In particular, at the "half-field" value of $B = 1500$ G a "forbidden" $\Delta S_z = 2$ line appears, accompanied by other lines attributable to various triplet systems (Figure 5a). These triplet spectra can be attributed to V^{4+}−V^{4+} ($S = 1$) pairs, for the tightest of which the approximate "point−dipole" model[29,30] would lead one to evaluate an interionic distance of ca. 0.26 nm (corresponding to a dipolar parameter of $D = 1500$ G). This indicates that V^{4+} ions are heterogeneously distributed in the zircon matrix. The cation−cation distances range between 0.291 and 0.3626 nm in the zircon structure. Therefore, some V^{4+} ions must be localized even in nearby positions in the lattice. This is in agreement with what was observed in ref 17 in the presence of ca. 0.1 V/Zr molar ratio, while no triplet line at all was reported in ref 12 in the presence of 0.06 V/Zr.

All these lines broaden with increasing V^{4+} concentration. Indeed, only an intense, ca. 140 G broad feature, appears at room temperature with the 0.1 V/Zr sample (Figure 5b). This band broadens at lower temperatures, resolving, at $T < 140$ K, again into a pattern similar to that of Figure 5a. This dependence of the spectral profile on the detection temperature indicates that V^{4+} ions interact with each other "dynamically", i.e. involving also lattice vibrations.
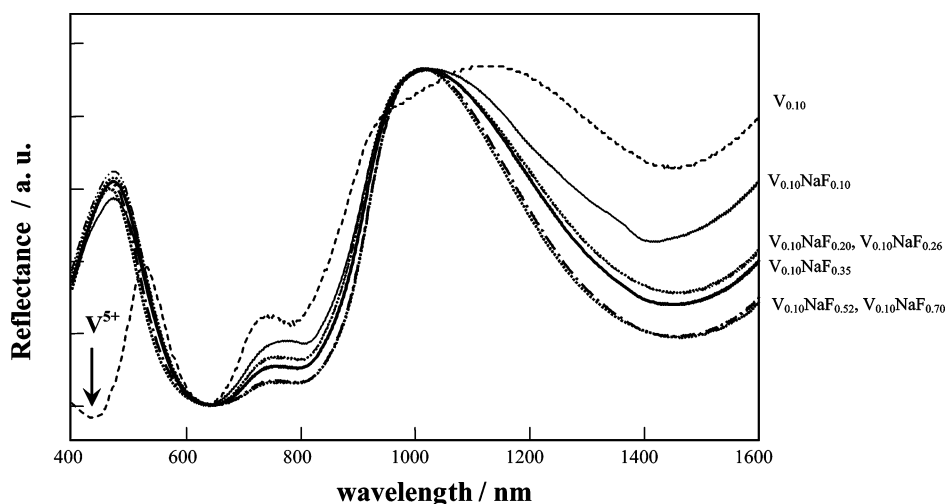
Figure 6. Diffuse reflectance spectra of 800 °C samples at variable NaF/Zr molar ratios and constant V/Zr content.

At even higher concentration of V_2O_5 the single feature narrows, assuming at room temperature a width of ca. 100 G in the case of the V_2O_5 0.14 V/Zr sample (Figure 5c).

Blue Samples. *UV−Vis Diffuse Reflectance Spectroscopy.* The addition of NaF in the sol−gel reaction mixture invariably promotes the development of the blue color of the pigment, whichever the specifically adopted conditions (vanadium content, temperature of calcinations, NaF amount). UV−vis diffuse reflectance spectra have been acquired on samples calcined at 800 °C containing the same V/Zr molar ratio (0.1) but different mineralizer amounts (Figure 6). The spectra are compared to the reference one obtained on the sample without NaF, which is characterized by a green color, while all the other samples are blue. All the spectra were scaled up with respect to the reflectance total variation.

The sample without NaF shows a minimum of reflectance at about 400 nm [31] due to V^{5+} not present in the blue samples. All the samples show (i) a signal at 640 nm [15] attributed to dodecahedral and tetrahedral V^{4+} coordination, (ii) a signal at 780 nm [5] due to a shoulder-forbidden transition of V^{4+}, and (iii) a signal a 1450 nm assigned to tetrahedral V^{4+} coordination.[31] It can be observed that by increasing the NaF content, the band at 1450 nm becomes more enhanced, while that one at 640 nm, attributed to both tetrahedral and dodecahedral V^{4+}, remains invariant. This could indicate that when the mineralizer concentration increases, the total amount of dodecahedral V^{4+} sites decreases since the total vanadium quantity is fixed. Unfortunately the signal attributed in the literature[32] to dodecahedral V^{4+} (300 nm)[32] is not detectable in our spectra because of the instrumental measurement range. These results are in total disagreement with the proposal by Llusar et al.,[31] who suggest that the mineralizers promote the substitution by V of Zr in the dodecahedral sites.

From the diffuse reflectance spectra L^*, a^*, and b^* parameters have been calculated. The obtained data are reported in Table 4. While the sample $V_{0.1}$ without the mineralizer is green (b^* small and positive), in the presence of NaF the b^* parameter is large and negative. Furthermore by addition of NaF the samples become also darker (L^*). The trend shown in Table 4, with regard to b^*, is confirmed by a literature study,[31] but the present samples are characterized by a more intense blue color.

Morphological Characterization. The development of the desired color is paralleled by several modifications in the features of the particles. Figure 7 reports the comparison between scanning electron microscopy (SEM) micrographs of

TABLE 4: CIE L^*, a^*, and b^* Parameters of 800 °C Heated Samples

sample	CIE		
	L^*	a^*	b^*
$V_{0.1}$	60.3	−16.9	2.7
$V_{0.1}NaF_{0.10}$	73.2	−19.7	−1.2
$V_{0.1}NaF_{0.20}$	66.2	−24.9	−22.3
$V_{0.1}NaF_{0.26}$	64.6	−25.2	−22.0
$V_{0.1}NaF_{0.35}$	60.0	−24.7	−23.4
$V_{0.1}NaF_{0.52}$	54.0	−21.7	−25.3
$V_{0.1}NaF_{0.70}$	53.7	−21.6	−28.3

two powders obtained in otherwise identical conditions except for the presence of NaF. The morphology of the particles appears strikingly different: in the absence of NaF the particles are much smaller (average size in the range of 100−200 nm) with a spheroidal or prismatic shape. In the presence of the mineralizer, instead, particles are much bigger and show a prismatic shape and relatively large size distribution.

Structural Characterization. Figure 8 reports, for samples calcined at 800 °C, the evolution of the zircon percentage and cell volume for increasing amounts of mineralizer in the synthesis. The zircon structure appears progressively promoted for amounts of NaF up to 0.25 molar ratio and then slightly decreases for larger contents. The unit cell volumes show in their turn a specular trend, first appreciably decreasing for amounts of NaF up to 0.26 and then showing a slight increase.

The promotion of the blue color by addition of the mineralizer has been largely reported in the literature, although the actual role played by the salt in the color promotion was never fully clarified. Monrós et al.[5] and Lusar et al.[31] report, consistently with the present results, a promotion of the zircon structure at lower temperatures, by addition of NaF, and a contraction of the unit cell volume. These authors interpret the contraction of the unit cell volume as being due to the partial substitution of O^{2-} in the lattice by smaller F^- ions. The promotion of the zircon structure in zircon pigments has been mainly attributed in the literature to the role played by fluorides in promoting the zircon formation by vehiculating "fluid" SiO_2 within the lattice of tetragonal zirconia.[7,8] In the case of yellow Pr pigments, however, we have observed[8] that, besides the possible role played by the F^-anion, the cationic partner of the salt played a relevant role in promoting the zircon structure, the promotion being more efficient for small monovalent cations and less efficient for large monovalent or divalent cations.

XANES Spectroscopy. Table 5 reports the preedge integral intensities obtained by fitting the preedge peak for samples
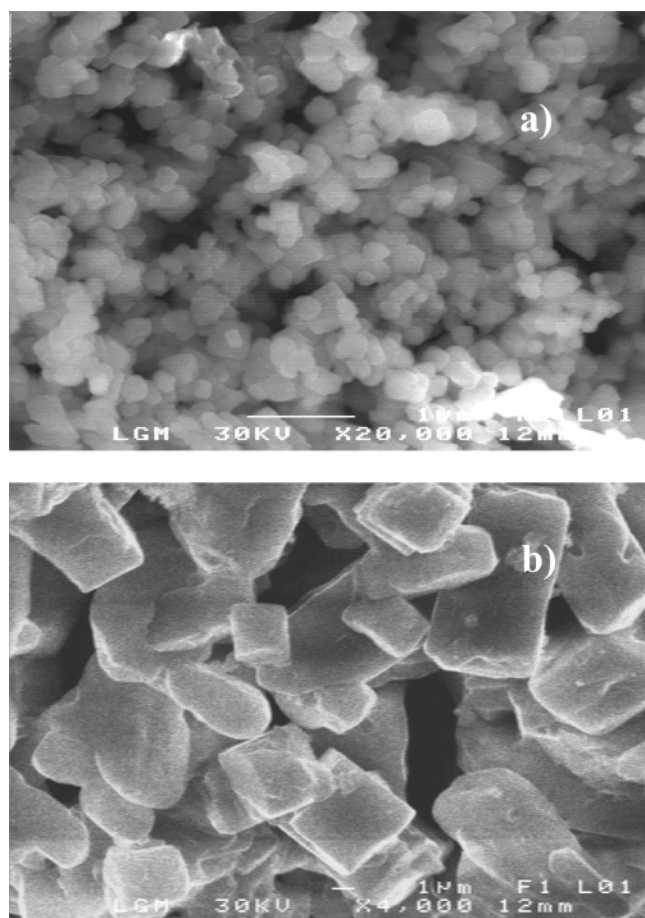
Blue, Vanadium-Doped ZrSiO$_4$ Pigments

J. Phys. Chem. B, Vol. 109, No. 47, 2005 **22117**

Figure 7. SEM images of 800 °C calcined samples (a) V$_{0.10}$ and (b) V$_{0.10}$NaF$_{0.26}$.
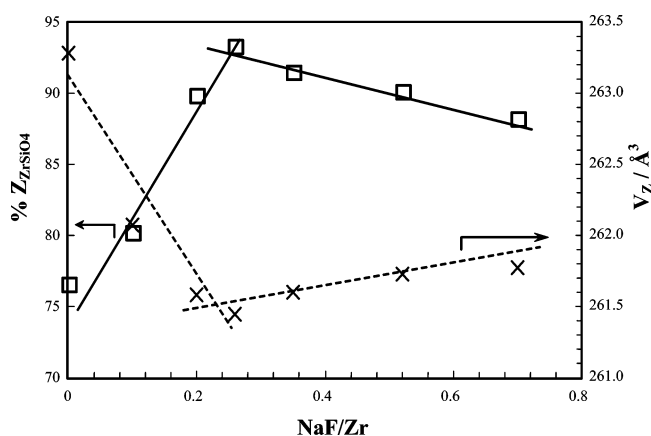

Figure 8. Zircon-phase mass percent (open squares) and relative cell volume (×) as a function of the NaF/Zr content at fixed V/Zr = 0.1.

obtained at constant vanadium content and increasing amounts of mineralizer. The intensity increases in passing from the sample with no mineralizer to the sample with the lowest NaF content and further progressively increases with the mineralizer concentration. The addition of NaF seems therefore to promote different locations of the V species in the zircon lattice. On the grounds of the discussion in the previous section and of literature data[26] an increase of the intensity should correspond to a decrease of the average V coordination number in the structure, or to a location in a site with lower symmetry.

EPR Spectroscopy. In Figure 9a the EPR spectrum of the "green sample" with 0.1 V/Zr (already shown in Figure 5b) is

TABLE 5: Spectral Characteristics of Preedge Peak in Samples Calcined at 800 °C at Different NaF/Zr Contents

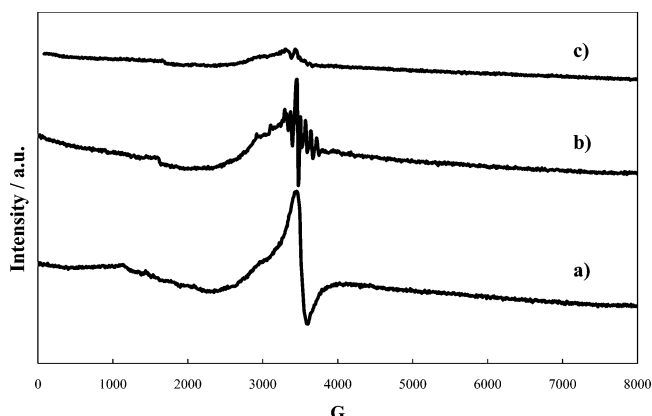|	preedge peak	
sample	energy position (eV)	integral intensity
V$_{0.1}$	5469.0	2954.3
V$_{0.1}$NaF$_{0.10}$	5469.1	3054.0
V$_{0.1}$NaF$_{0.20}$	5469.1	3069.7
V$_{0.1}$NaF$_{0.26}$	5469.0	3097.7
V$_{0.1}$NaF$_{0.35}$	5469.0	3036.2
V$_{0.1}$NaF$_{0.52}$	5469.0	3184.4
V$_{0.1}$NaF$_{0.70}$	5469.0	3392.1

Figure 9. EPR spectra of ZrSiO$_4$ with V/Zr = 0.1 and NaF/Zr of (a) 0.00, (b) 0.26, and (c) 0.70.
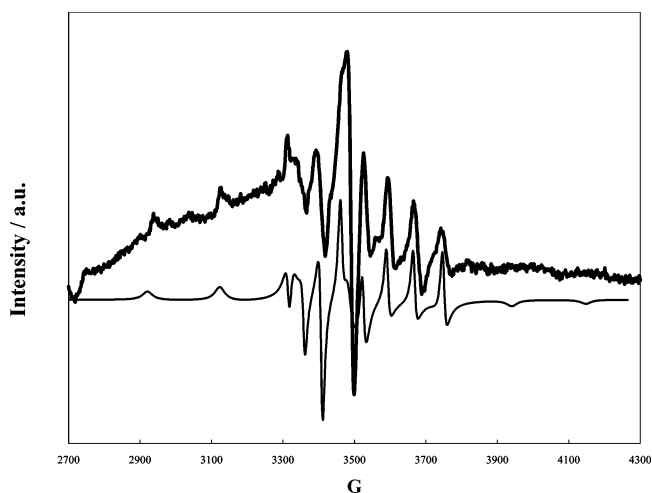

Figure 10. EPR spectrum of ZrSiO$_4$ with V/Zr = 0.1 and NaF/Zr = 0.26. Thinner line: simulation with the parameters reported in Table 1.

compared to those obtained with the "blue samples" characterized by the same V amount but containing also 0.26 NaF/Zr (Figure 9b) and 0.70 NaF/Zr (Figure 9c) molar ratios. The spectrum of Figure 9b is completely different from that of Figure 9a. Indeed, it has been simulated (Figure 10) by attributing it to isolated V^{4+} ions characterized by the magnetic parameters reported in Table 6. Of course, it was not surprising that isolated V^{4+} ions resulted on diluting V^{4+} clustered ions by NaF. This spectrum was detectable at least up to 300 K in agreement with the spectra reported by Torres et al.[1] in the case of V-doped tetragonal zirconia; in this latter case vanadium was considered to be present in octahedral geometry with strong tetragonal distortion. The present results appear, instead, to be at variance with results reported by Di Gregorio et al.[12] and Ocana et al.[17] obtained only at very low temperatures, in the case of V-doped ZrSiO$_4$ with a lower mineralizer content.

TABLE 6: EPR Parameters of Literature and Present Samples at Different V/Zr Contents and with Addition of the Mineralizer NaF

sample (different T)	ref	phase	$g_\perp$	$g_\parallel$	$A_\perp$/G	$A_\parallel$/G	T/K
$V_{<0.04}$	1	t-ZrO$_2$	1.942	1.927	76	151	10
$V_{0.04}$	1	t-ZrO$_2$	1.980	1.920	65	180	298
$V_{0.06}$	33	ZrSiO$_4$	1.970	1.893	31	87	20
	12	ZrSiO$_4$		1.889	31	90	4
$V_{0.10}NaF_{0.13}$	17	ZrSiO$_4$	1.970	1.893	31	88	15
$V_{0.10}NaF_{0.26}$	present work	ZrSiO$_4$	1.975	1.923	62	205	300

Furthermore, the hyperfine parameters found by us in the case of the 0.26 NaF/Zr sample are comparable to the ones reported at room temperatures for V in tetragonal zirconia,[1] but they are nearly twice those reported in the literature[12,17] for V in zircon (see Table 6).

Therefore a different paramagnetic system is observed in the case of the present, NaF added, V-doped zircon samples.

Discussion

Green Samples. The different characterizations, performed on the samples obtained in the absence of mineralizers (green samples), present some general trends which may be commented on with respect to previous literature results. Structural data show that the unit cell volume of the V-doped powders is, in any case, expanded with respect to the undoped zircon cell; furthermore, the presence of vanadium appears to increasingly promote the zircon structure up to about V/Zr = 0.05, while larger metal amounts do not appreciably modify the samples phase composition. The percent amount of the zircon phase can be increased by two different ways: by increasing the heating temperature, while keeping constant the amount (e.g. 10%) of V substituting for Si (Figure 1), or by increasing the amount of V substituting for Si, while keeping constant the heating temperature (e.g. 1000 °C) (Table 2). In the former case the cell volume V_Z decreases, though remaining greater than for the undoped zircon (Figure 2). By contrast, in the latter case the cell volume increases, though only up to the limit of V "solubility" (Table 2 and Figure 3). Therefore, the increasing of the cell volume is not a consequence of the increased amount of zircon phase, but, on the contrary, it is produced by the substitution of Si by V, up to the solubility limit of the last. Indeed, several data are reported in the literature concerning the solubility limit of vanadium in ZrSiO$_4$. Values in the V/Zr range of 0.01–0.05 are reported on the grounds of diverse experimental evidence or for samples obtained by different experimental routes. Torres et al.,[25] on the basis of a Rietveld refinement study of X-ray diffraction data, conclude that V^{4+} is uniquely located in the tetrahedral sites up to amounts of nominal vanadium of 0.04. For higher vanadium loadings, i.e., for V/Zr = 0.2, the Zr^{4+} occupying the dodecahedral site is substituted for by V^{4+}. The authors do not report data for vanadium amounts in the range between 0.04 and 0.2. The present structural data may be in agreement with the conclusions by Torres et al. as the observed promoting role of the metal may coincide with the lattice substitution of Si^{4+}. However if the other, present, characterizations are considered, the picture becomes less straightforward.

The trend of the intensity of the preedge peak in X-ray absorption spectra can be used to obtain information concerning the localization of the metal in the zircon lattice. A decrease in the preedge peak intensity can be attributed to an increase in the coordination number of the metal, i.e., to a transition from a prevailing tetrahedral coordination (substitution in the Si^{4+} sites) to the dodecahedral symmetry pertaining to Zr^{4+} substitu-

tion. Data in Table 3 show that the intensities progressively decrease with the V content, presenting a marked drop for vanadium amounts larger than about 0.04. It appears, therefore, that for metal dopings larger than about 0.05, additional vanadium can be considered to be mainly localized in the dodecahedral sites of Zr^{4+} in agreement with literature results. However the slight decrease of the intensity already apparent at the lowest vanadium loadings may suggest that V species, although being mainly localized in the tetrahedral Si positions, may also occupy to a much lesser extent the Zr lattice positions, even for vanadium amounts lower than 0.05.

Support to this latter hypothesis may be, possibly, sought from the analysis of EPR spectra. A triplet EPR spectrum is appreciable for vanadium amounts of 0.02, while at 0.1 the spectrum is of a different kind. Di Gregorio et al.[12] have suggested that the ESR of V–ZrSiO$_4$, in which V occupies the tetrahedral Si sites, is only observable at very low temperatures due to a dynamic Jahn–Teller effect which, in turn, provokes Orbach relaxation. If this were the case, the triplet observed at room temperature for the sample at the lowest V loading could be the result of a substitution of Zr by V in the dodecahedral environment accompanying the principal Si substitution, already at the lowest vanadium loadings.

Blue Samples. The addition of NaF to the sol-reacting mixture provokes several manifest effects, the most striking being the turning of the greenish color of the powders to an intense blue. The contraction of the unit cell volume observed by us, with respect to the V-doped samples in the absence of NaF, in agreement with previous results, is interpreted in the literature as being the result of the substitution of oxygen in the lattice by smaller F$^-$ ions. Although this hypothesis cannot be excluded, other possibilities must be taken into account.

The scaling-up of UV–vis diffuse spectra suggests that the addition of the mineralizer supports the promotion of vanadium in a tetrahedral coordination site. Amounts of V around 0.05 represent a limit for the tetrahedral Si substitution. Some authors[1] suggest that the presence of the mineralizer could support incorporation of larger vanadium amounts into the zircon lattice. Alternatively a tetrahedral location of V, different from the Si substitution, can be considered.

In fact EPR spectra show that a different paramagnetic system occurs upon mineralizer addition.

The progressive increase in the intensity of the preedge XANES peak suggests that the addition of NaF provokes the localization of V in sites bearing lower coordination or lower symmetry with respect to the sites occupied in the absence of NaF. It is the opinion of the authors that the addition of the mineralizer provokes the localization of V into the interstitial, strongly distorted tetrahedrally coordinated site 16g with site symmetry[18,19] C_2 (Figure 11). The symmetry of this site is lower that that pertaining to both Zr and Si substitutional sites, D_{2d}, and, therefore, a prevailing location of the metal in this interstitial position could support the increase in the intensity
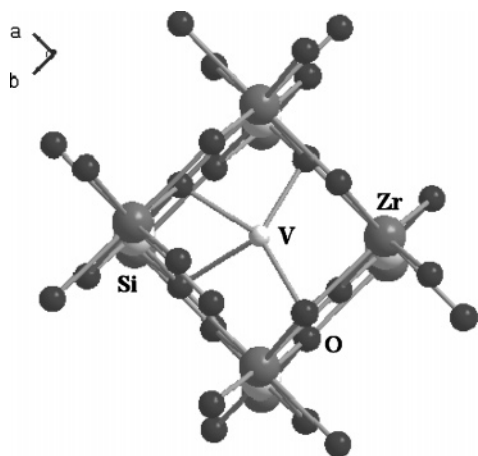
Blue, Vanadium-Doped ZrSiO$_4$ Pigments

J. Phys. Chem. B, Vol. 109, No. 47, 2005 **22119**

Figure 11. Sketch of zircon structure along [001], showing the strongly distorted tetrahedrally coordinated interstitial site, V$_{int}$.

of the preedge XANES peak and rationalize, jointly, all the reported evidence concerning the blue samples.

Conclusions

V-doped zircon samples are obtained by following a sol−gel procedure combined with thermal treatments performed in the range of 600−1200 °C.

The formation of the zircon phase appears to be promoted by increasing the V loading in the powders up to 0.05 V/Zr molar ratios. This vanadium amount can be considered as a threshold value with respect to the localization of V in the lattice. For vanadium amounts lower than 0.05, the metal is prevailingly substituted to Si in the tetrahedral positions of the lattice, while for loadings larger than 0.05, additional V is only localized in the Zr^{4+} dodecahedral positions of the lattice.

In the "green samples" obtained in the absence of mineralizer, vanadium is present both as V^{5+} and V^{4+} species. The addition of NaF to the sol−gel starting mixture invariably promotes the blue color of the pigment; this effect is due to the sole presence of V^{4+} species in the system. Results, by the different characterizations jointly indicate that the addition of NaF, besides promoting the blue color and the zircon structure, causes the localization of V in sites with lower symmetry with respect to the case of the green samples. To the authors' knowledge, no such evidence was previously reported in the literature. The localization of V species in the interstitial strongly distorted position with C_2 symmetry is proposed to take place upon NaF addition to the system.

References and Notes

(1) Torres, F. J.; Folgado, J. V.; Alarcon, J. *J. Am. Ceram. Soc.* **2002**, *85*, 794.
(2) Ocana, M.; Caballero, A.; Gonzalez-Elipe, A. R.; Tartaj, P.; Serna, C. J.; Merino, R. I. *J. Eur. Ceram. Soc.* **1999**, *19*, 641.
(3) Tartaj, P.; Gonzalez-Carreno, T.; Serna, C. J.; Ocana, M. *J. Solid State Chem.* **1997**, *128*, 102.
(4) Ardizzone, S.; Binaghi, L.; Cappelletti, G.; Fermo, P.; Gilardoni, S. *Phys. Chem. Chem. Phys.* **2002**, *4*, 5683.
(5) Monrós, G.; Carda, J.; Tena, M. A.; Escribano, P.; Sales, M.; Alarcón, J. *J. Europ. Ceram. Soc.* **1993**, *11*, 77.
(6) Ocana, M.; Caballero, A.; Gonzalez-Elipe, A. R.; Tartaj, P.; Serna, C. J. *J. Solid State Chem.* **1998**, *139* (2), 412.
(7) Cappelletti, G.; Ardizzone, S.; Fermo, P.; Gilardoni, S. *J. Eur. Ceram. Soc.* **2005**, *25*, 911.
(8) Del Nero, G.; Cappelletti, G.; Ardizzone, S.; Fermo, P.; Gilardoni, S. *J. Eur. Ceram. Soc.* **2004**, *24*, 3603.
(9) Seabright, C. A. U.S. Pat. 2441447, 1948.
(10) Demiray, T.; Nath, D. K.; Hummel, F. A. *J. Am. Ceram. Soc.* **1970**, *53*, 1.
(11) Beltran, A.; Bohm, S.; Flore-Riveros, A.; Igualada, J. A.; Monros, G.; Andres, J.; Luana, V.; Martin Pendas, A. *J. Phys. Chem.* **1993**, *97*, 2555.
(12) Di Gregorio, S.; Greenblatt, M.; Pifer, J. H.; Sturge, M. D. *J. Chem. Phys.* **1982**, *76*, 2931.
(13) de Waal, D.; Heyns, A. M.; Pretorius, G.; Clark, R. J. H. *J. Raman Spectrosc.* **1996**, *27*, 657.
(14) Wertz, J. E.; Bolton, J. R. *Electron Spin Resonance. Theory and Applications*; McGraw-Hill: New York, 1972; p 288.
(15) Xiayou, H.; Gui-Ku, B.; Min-Guang, Z. *J. Phys. Chem. Solids* **1985**, *46*, 719.
(16) Chandley, P.; Clark, R. J. H.; Angle, R. J.; Price, G. D. *J. Chem. Soc., Dalton Trans.* **1992**, *1992*, 1579.
(17) Ocana, M.; Gonzalez-Elipe, A. R.; Orera, V. M.; Tartaj, P.; Serna, C. J.; Merino, R. I. *J. Am. Ceram. Soc.* **1998**, *81*, 395.
(18) Siggel, A.; Jansen, M. *Z. Anorg. Allg. Chem.* **1990**, *583*, 67.
(19) Niesert, A.; Hanrath, M.; Siggel, A.; Jansen, M.; Langer, K. *J. Solid State Chem.* **2002**, *169*, 6.
(20) Dajda, N.; Dixon, J. M.; Smith, M. E.; Carthey, N.; Bishop, P. T. *Phys. Rev. B: Condens. Matter Mater. Phys.* **2003**, *67*, 024201.
(21) Larson, A. C.; Von Dreele, R. B. *GSAS: General Structural Analysis System*; Los Alamos National Laboratory: Los Alamos, NM, 1994.
(22) Toby, B. H. *J. Appl. Crystallogr.* **2001**, *34*, 210.
(23) Tartaj, P.; Serna, C. J.; Ocana, M. *J. Am. Ceram. Soc.* **1995**, *78*, 1147.
(24) Domenech, A.; Torres, F. J.; Alarcon, J. *Electrochim. Acta* **2004**, *49*, 4623.
(25) Torres, F. J.; Tena, M. A.; Alarcon, J. *J. Eur. Ceram. Soc.* **2002**, *22*, 1991.
(26) Wong, J.; Lytle, F. W.; Messmer, R. P.; Maylotte, D. H. *Phys. Rev. B: Condens. Matter Mater. Phys.* **1984**, *30*, 5596.
(27) Tanaka, T.; Yamashita, H.; Tsuchitani, R.; Funabiki, T.; Yoshida, S. *J. Chem. Soc., Faraday Trans. 1* **1988**, *84*, 2987.
(28) Anpo, M.; Higashimoto, S.; Matsuoka, M.; Zhanpeisov, N.; Shioya, Y.; Dzwigaj, S.; Che, M. *Catal. Today* **2003**, *78*, 211.
(29) Marshall, W. In *Paramagnetic Resonance*; Low, W., Ed.; Academic Press: New York, 1963.
(30) Hutchinson, C. A.; McKay, D. B. *J. Chem. Phys.* **1977**, *66*, 3311.
(31) Lusar, M.; Vicent, J. B.; Badenes, J.; Tena, M. A.; Monros, G. *J. Eur. Ceram. Soc.* **1999**, *19*, 2647.
(32) Valentin, C.; Munoz, M. C.; Alarcon, J. *J. Sol-Gel Sci. Technol.* **1999**, *15*, 221.
(33) Ball, D.; Wanklyn, B. *Phys. Status Solidi A* **1976**, *36*, 307.